UNRAVELING THE STRUCTURE OF THE RIBOSOME

Nobel Lecture, December 8, 2009

by

V. RAMAKRISHNAN

MRC Laboratory of Molecular Biology, Hills Road, Cambridge CB2 0QH, United Kingdom.

INTRODUCTION

During the decade following the discovery of the double-helical structure of DNA, the problem of translation, namely how genetic information is used to synthesize proteins, was a central topic in molecular biology. A crucial idea, proposed by Crick (1955), was that a small intermediary molecule containing a tri-nucleotide that base-paired with the genetic template would bring along a covalently linked amino acid for addition to the polypeptide chain. This idea, called the "adapter hypothesis," was soon confirmed when a "soluble" or "s" RNA was discovered that had covalently linked amino acids (Hoagland *et al.,* 1958; for a retrospective, see Hoagland, 2004). It is sad to note that two of the key scientists involved in this work, Hoagland and Zamecnik, both died in the fall of 2009 around the time when the Nobel Prize for the ribosome was announced. The sRNA, renamed tRNA, is a central player in the process of translation. Unlike the trinucleotide originally envisioned, it actually consists of about 76 nucleotides (Holley *et al.,* 1965), with the anticodon end that recognizes the triplet codon on mRNA about 75 Å away from the 3′ end that has the covalently linked amino acid (Robertus *et al.,* 1974; Kim *et al.,* 1974).

At the same time, scientists studying the ultrastructure of the cell noticed that newly synthesized proteins were localized in particles on the endoplasmic reticulum (Palade and Siekevitz, 1956), suggesting that a large complex assembly was involved in the process of translation. These particles could be isolated and were originally called the "ribonucleoprotein particles of the microsomal fraction." Fortunately, at an early meeting, Howard Dintzis proposed that the particle be called the "ribosome" and the name has been used ever since (Dintzis, 2006).

Decades of subsequent work established a number of salient facts such as the shape of ribosomes, their composition, the number of tRNA binding sites, the main roles of the two subunits and the involvement of protein factors, many of them GTPases, at specific stages of translation (for background, see the volume edited by Nomura *et al.,* 1974). Ribosomes from all species consist of two subunits that dissociate reversibly (Chao, 1957; Tissières and

Watson, 1958). The subunits of the 70S bacterial ribosome are designated 30S and 50S, whereas those of the 80S eukaryotic ribosome are designated 40S and 60S after their respective sedimentation coefficients. The small subunit binds mRNA and the anticodon stem loops of tRNA. The large subunit contains the peptidyl transferase center where catalysis of the peptide bond formation occurs. In both bacteria and eukaryotes, the ribosome is about 2/3^{rds} RNA and 1/3rd protein by mass, although in mammalian mitochondria, this ratio is reversed (Hamilton and O'Brien, 1974).

I began studying ribosomes as a postdoctoral fellow in Peter Moore's laboratory in 1978. There I participated in a project to determine the spatial location of the 30S proteins by neutron scattering, which culminated in the so-called "neutron map" (Capel *et al.,* 1987). In 1983, I joined the Biology Department at Brookhaven National Laboratory as a staff scientist, and just two years later, Stephen White, who had moved from Wittmann's department at the Max Planck Institute for Molecular Genetics in Berlin joined me as a colleague. He had brought with him several crystallization projects of individual ribosomal proteins. I decided to use the then new more highly regulated version of the T7 expression system (Studier *et al.,* 1990), which allowed us to clone the genes for and overexpress many of these proteins (Ramakrishnan and Gerchman, 1991). We used this system to make large quantities of almost any desired ribosomal protein, and to label them with cysteines (for mercury derivatives) or with selenomethionine. The result was that after a long hiatus, the pace of determination of structures of ribosomal proteins increased quickly (Ramakrishnan and White, 1998). However, it gradually became clear that these structures by themselves would not be ultimately useful in understanding ribosome function, even when used as labeling markers for footprinting studies or in modeling into electron microscopy (EM) maps of the ribosome. Only the high-resolution structures of entire ribosomal subunits or the whole ribosome would suffice.

The first indication that ribosomes were identical molecules that could be packed into a crystalline lattice came from the observation of naturally occurring two-dimensional crystalline arrays (Unwin and Taddei, 1977). However, a major breakthrough was achieved when Yonath, Wittmann and their coworkers produced the first three-dimensional crystals of the 50S subunit from *Bacillus stearothermophilus* (Yonath *et al.,* 1980). After nearly a decade of work and the exploration of other species, in another landmark, Yonath and coworkers obtained crystals of the 50S from *Haloarcula marismortuii* that diffracted to 3 Å resolution (von Böhlen *et al.,* 1991), suggesting that an atomic structure of the subunit would be possible if the crystallographic difficulties could be overcome. Another major contribution was made by the group of Marina Garber in the Institute for Protein Research in Puschino, Russia. They reported the first single crystals of both the 30S subunit and the 70S ribosome from *Thermus thermophilus* (Trakhanov *et al.,* 1987; Yusupov *et al.,* 1987). Similar crystals of the 30S subunit from the same species were subsequently obtained by Yonath and coworkers (Yonath *et al.,* 1988). Finally, in a crucial technical advance, Hope had shown that data

collection at 100 K minimized radiation damage for several proteins (Hope, 1988) and he and Yonath collaborated to show that this method allowed data collection from crystals of ribosomal subunits (Hope *et al.,* 1989).

DETERMINING THE STRUCTURE OF THE 30S SUBUNIT

Thus in 1995, when I moved to the University of Utah, well-diffracting crystals of the 50S subunit had existed for some time, but with limited progress on determining its structure. However, there were no crystals of the 30S subunit that diffracted to high resolution. Given my longstanding interest in ribosomes and in the 30S subunit in particular, I therefore decided to try and obtain good crystals of it with the goal of determining its structure. At about this time, Joachim Frank and coworkers had helped to develop the use of single particle reconstruction methods in conjunction with cryoelectron microscopy (cryoEM). In their studies, they found that the conformation of the 30S subunit was different in inactive, active and 50S-bound states (Lata *et al.,* 1996). This suggested that the difficulty in obtaining well-diffracting crystals might be due to the conformational variability of the 30S subunit. We had recently solved the isolated structure of initiation factor IF3, which was thought to bind one of the regions of the 30S subunit that was conformationally variable (Biou *et al.,* 1995). Accordingly, we started with the idea that the binding of IF3 to the 30S subunit might fix the latter in a single conformation suitable for producing better crystals. We began by initiating a collaboration with Joachim Frank and Raj Aggrawal to determine a cryoEM structure of the complex of IF3 with the 30S subunit (McCutcheon *et al.,* 1999). Although later studies showed that our interpretation of the density in terms of the domains of IF3 was only partly correct (Dallas and Noller, 2001; Allen *et al.,* 2005), the difference density nevertheless clearly showed that IF3 bound to the conformationally variable platform region of the 30S subunit. We therefore set about trying to crystallize the 30S subunit in complex with IF3. It is just as well that we did not need a complex with IF3 to determine the structure of the 30S subunit or we would still be waiting.

To begin with, we decided to reproduce the low-resolution crystals from *Thermus thermophilus* obtained earlier by the Puschino group (Trakhanov *et al.,* 1987; Yusupov *et al.,* 1987) because that would tell us whether our ribosome preparations were good enough to crystallize. Marina Garber, who led the group that crystallized the 30S subunit and 70S ribosomes in Puschino, told us that the use of hydrophobic chromatography was useful to get ribosomes that were good enough to produce 70S crystals. I had some previous experience in the use of this method to make ribosomes (Ramakrishnan *et al.,* 1986), so with the help of Bob Dutnall, a postdoc working on histone acetyltransferases, I tested a number of different hydrophobic resins before settling on the Poros-ET column made by Biocad (Clemons *et al.,* 2001).

We obtained initial crystals of the 30S subunit within a few months. These crystals lacked ribosomal protein S1 (Fig. 1A), which is present in variable stoichiometry in preparations of the 30S subunit. Although we could get large crystals even from this heterogeneous preparation, the reproducibility and size improved significantly when we systematically removed S1 quantitatively prior to crystallization (Fig. 1B), and these crystals diffracted to beyond 3 Å resolution (Fig. 1C) (Clemons *et al.,* 1999; Clemons *et al.,* 2001). Thus we had in hand crystals that were in principle capable of yielding an atomic structure of the 30S subunit provided we could collect complete data to the resolution limit and solve the phase problem.

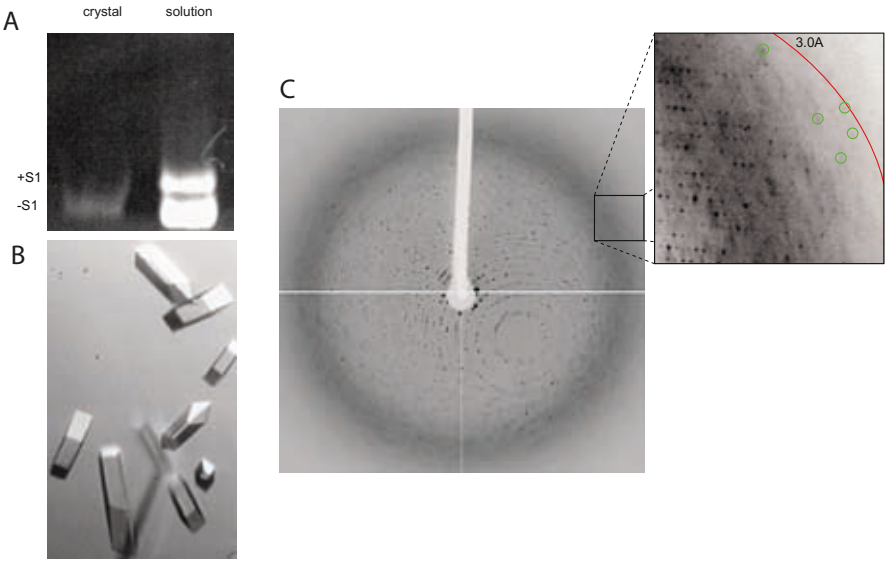

Figure 1. A. An agarose-acrylamide non-denaturing gel of redissolved crystal of the 30S ribosomal subunit (showing they lack protein S1) and the input sample that contained a mixture of 30S subunits with and without protein S1. B. Crystals of 30S subunits. C. Diffraction from the crystals in B, showing spots to about 3 Å resolution.

When we began, the difficulties of obtaining good phases for ribosome-sized molecules had been apparent for some time, and it was clear that the field could use fresh ideas. Only a few years earlier, I had used the technique of multiwavelength anomalous diffraction (MAD) pioneered by Wayne Hendrickson and Keith Hodgson (Phillips and Hodgson, 1980; Hendrickson *et al.,* 1988) in conjunction with the use of incorporated selenomethionine as an anomalous scatterer (Hendrickson *et al.*, 1990) to solve the structure of the globular domain of histone GH5 (Ramakrishnan *et al.,* 1993). In the process of solving that structure, following an initial suggestion by Eleanor Dodson, I had shown that the treatment of MAD data as a special case of multiple isomorphous replacement with anomalous scattering produced excellent maps, which was surprising considering the very low anomalous and

dispersive signal of a few electrons from a selenium atom (Ramakrishnan *et al.,* 1993; Ramakrishnan and Biou, 1997). The reason for this is that although both the anomalous and dispersive signals from selenium are only a few electrons rather than the ~80 electrons of a "heavy" atom like gold or mercury, there is far less noise from scaling or nonisomorphism in MAD, so that the signal to noise is actually much better than that of a typical solution using isomorphous replacement.

This naturally led me to ask what it would take to have sufficient anomalous scattering to produce a measurable signal from crystals of a 30S subunit. A back of the envelope calculation in conjunction with Ethan Merritt's web site that calculates the expected signal (http://skuld.bmsc.washington.edu/scatter/AS_signal.html) showed that there were too few methionines in the 30S subunit to provide a measurable signal. At the IUCr meeting in Seattle in 1996, Wayne Hendrickson described the enormous signals from the M4 or M5 edges of uranium (Liu *et al.,* 2001), whose anomalous scattering could be as much as 100 electrons. However, a conversation with Craig Ogata, who had carried out these experiments, made me realize that the technical difficulties of carrying out such an experiment would be enormous because of the wavelengths required and the consequent radiation damage. A reasonable compromise was the use of the LIII edges of lanthanides that had produced spectacular maps (Weis *et al.,* 1991). A calculation showed that as few as 10–20 well-bound lanthanide sites would yield a sufficiently strong anomalous signal to derive phase information from the 30S subunit. A paper on the cleavage of ribosomal RNA by lanthanides in alkaline pH suggested that there were indeed a number of well defined sites for lanthanides in the 30S subunit (Dorner and Barta, 1999). We therefore decided to embark on trying to phase the 30S subunit using anomalous scattering from the LIII edges of lanthanides. I believed that we would probably be able to locate the anomalous scatterers using direct methods, and tests done after the fact suggested that indeed this would have been the case.

As we embarked on this, two developments occurred that influenced our course of action. The first, in 1996 was the publication of the P4-P6 domain of the group I intron (Cate *et al.,* 1996) which was solved using MAD from an LIII anomalous edge. The compound that contributed most to phasing of this large RNA was osmium hexamine. It was clear from the characteristics of its binding site (Cate and Doudna, 1996) that this compound would probably bind to many more sites in the 30S subunit than most lanthanides. However, it was not commercially available, and since Henry Taube, who had provided the compound to the authors of the P4-P6 study, no longer had any of it to spare, I asked my friend and former colleague at Brookhaven, Bruce Brunschwig (now at Caltech), if he could make it for me. He very kindly agreed and with his associate Mei Chou made enough for our studies.

The other development was the publication of the 9 Å structure of the 50S subunit from Yale (Ban *et al.,* 1998), which for the first time showed right-handed helices for double-stranded RNA, which was a major breakthrough.

To obtain this, they had used heavy atom tungsten clusters, previously suggested by Yonath and coworkers (Thygesen *et al.*, 1996). However, they had also obtained starting phases from molecular replacement using a cryoEM reconstruction of the 50S subunit done by Joachim Frank and his colleagues as a starting model. The W18 cluster was directly visible in difference Patterson maps, so it is not clear that molecular replacement phases from a cryoEM model was actually required, but they were able to confirm the location of the W18 clusters using difference Fourier maps from those phases. Accordingly, we decided to try both molecular replacement using cryoEM and use heavy atom clusters as a way of obtaining starting phases from which we could locate our anomalous scatterers at LIII edges by difference Fourier methods. We obtained a set of tungsten clusters ranging from 11 to 26 atoms from Michael Pope of Georgetown University, who generously sent them to us, as he had previously to Yonath and Steitz. A different cluster, tantalum bromide, was kindly provided by Gunther Schneider of Stockholm University and from Jan Löwe, whom I joined as a colleague at the MRC Laboratory of Molecular Biology in Cambridge soon after collecting the data described in the following paragraph.

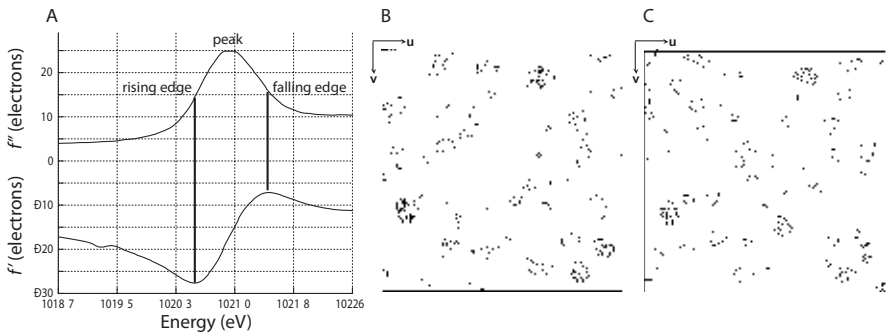

Figure 2. A. Spectrum of the LIII edge of tungsten, courtesy of S. Myers and D. Schneider, Brookhaven National Laboratory. Data were initially collected at the peak of *f*" where the anomalous differences are maximized, and subsequently at the two wavelengths that correspond to the minimum and local maximum of *f'*. B. Harker section of anomalous difference Patterson map of a W17 derivative of the 30S crystals, generated from the data at the peak of *f*" showing peaks corresponding to the W17 clusters in the structure. C. Harker section of Patterson maps of the isomorphous (dispersive) difference between the data collected at the minimum and local maximum of *f'*, showing peaks at identical locations as in B.

Attempts at molecular replacement using cryoEM reconstructions of the 30S subunit at ~25 Å resolution provided by Joachim Frank as a starting model did not yield a solution in our hands. However, during a single trip to the NSLS at Brookhaven, we collected data at the peak of the fluorescence spectrum at the LIII edges for the various tungsten clusters, tantalum bromide, and lanthanides as well as osmium hexamine. The peak corresponds to the maximum of *f*" (Fig. 2A), resulting in maximizing anomalous

differences between Bijvoet pairs. Even while at the beamline, we could see clear anomalous difference Patterson peaks for the W17 cluster (Fig. 2B). We accordingly collected two more wavelengths on this derivative to maximize the dispersive signal by collecting at the "rising edge" and "falling edge" of the fluorescence spectrum. These very close wavelengths correspond to the minimum and local maximum of the real part *f'* of the anomalous scattering factor, and by choosing them, we maximized the dispersive or "isomorphous" difference in *f'* between the two wavelengths, which resulted in strong peaks for the difference Patterson at the same positions as those for the anomalous difference (Fig. 2C). Using both the dispersive and anomalous differences in MAD phasing yielded us initial phases to about 9 Å resolution. We used these phases to locate all of the other derivatives. Because the various derivatives were not isomorphous with one another, we grouped together those derivatives that were isomorphous to medium resolution to solve the structure of the 30S to 5.5 Å resolution (Clemons *et al.,* 1999).

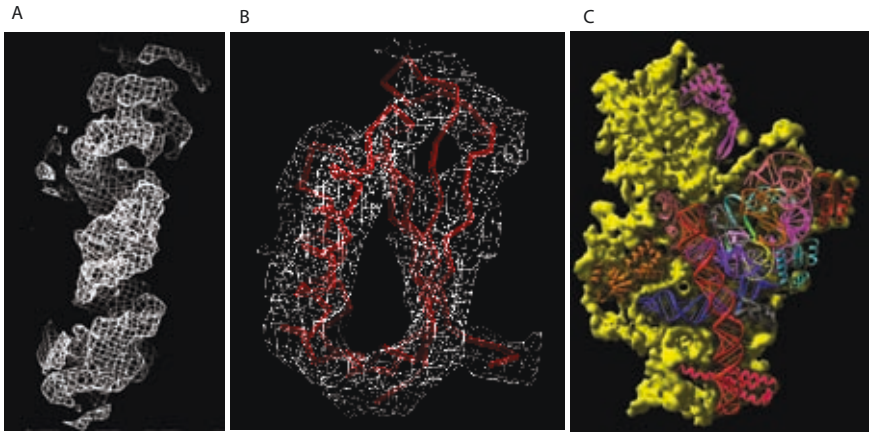

Figure 3. The 5.5 Å structure of the 30S subunit. A. Density for right-handed double helical RNA showing the two strands and bumps for the phosphate groups. B. Density for ribosomal protein S6, showing the fit of the isolated protein structure (Lindahl *et al.,* 1994). C. A partial model of the 30S subunit in which the fold of the central domain has been traced, and all proteins of previously known structure as well as S20 had been placed in the electron density. Reproduced from Clemons *et al.* (1999).

This structure represented a breakthrough in several respects. It showed that reliable phases could be obtained with our 30S subunit crystals. We could clearly see double-helical density for RNA and recognize the long penultimate helix 44 of 16S RNA at the interface (Fig. 3A). Because the resolution was sufficiently high to recognize individual proteins of known structure (Fig. 3B), we were able to place all of the 30S proteins whose structure was previously known, as well as protein S20, which was a three-helical bundle at the "bottom" of the subunit. Finally, in conjunction with biochemical data, especially footprinting data from Noller and coworkers (Stern *et al.,* 1989; Powers and Noller, 1995), we were able to identify stretches of RNA adjacent

to specific proteins and thereby trace the fold of most of the central domain, resulting in a partial model for the 30S subunit (Fig. 3C). Since the crystals diffracted to ~3 Å, the way to an eventual atomic structure seemed clear.

Unfortunately, the progress to high resolution was beset by several problems. Because the diffraction at high resolution was quite weak, it became necessary to take much longer exposures in order to obtain sufficiently accurate data to the resolution limit. However, the crystals suffered from sensitivity to radiation damage at these higher exposures, requiring multiple crystals for a complete data set. At the same time, they showed variability in cell dimensions resulting in non-isomorphism which made it impossible to scale data together from multiple crystals. These two mutually incompatible problems made it difficult for us to make progress for several months. The problem was solved partly by brute force in which we screened hundreds of crystals and grouped them into sets that had similar cell dimensions. We also noticed that crystals soaked in osmium hexamine seemed to have consistent cell dimensions, and decided to soak all crystals in the isostructural cobalt hexamine, which greatly reduced crystal-to-crystal non-isomorphism. The structure was solved using mainly anomalous scattering from a variety of lanthanides and osmium hexamine at their respective LIII edges. In hindsight, we found that anomalous scattering from just the osmium hexamine derivative in conjunction with density modification would have given us equally good phases. Given his prior work on the P4-P6 domain, it is not surprising that Cate independently adopted an essentially identical strategy of anomalous scattering from osmium or iridium hexamine for the solution of the 5.5 Å structure of the 70S ribosome in the Noller laboratory (Cate *et al.,* 1999; Yusupov *et al.,* 2001), and it was also essential for solving the 50S subunit to high resolution (Ban *et al.,* 2000).

THE STRUCTURE OF THE 30S SUBUNIT

We finally succeeded in solving the atomic structure of the 30S subunit from *Thermus thermophilus* and an essentially complete atomic model that included all the RNA and proteins present was refined to 3 Å resolution (Wimberly *et al.,* 2000) (Fig. 4). At about the same time, the Yonath group, using slightly different methods and using crystals that required the binding of heavy atom clusters to diffract well, independently solved a structure of the 30S subunit to 3.3 Å (Schluenzen *et al.,* 2000). This structure, besides being less complete, had a number of discrepancies with our structure (detailed in Brodersen *et al.,* 2002), but a subsequent structure published by that group the following year (Pioletti *et al.,* 2001) at 3.2 Å agreed well with our original structure.

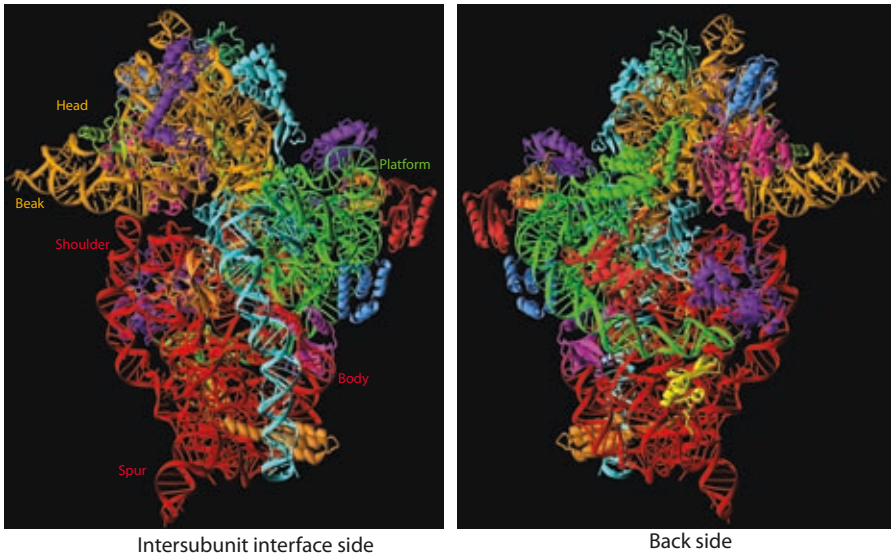

Figure 4. The atomic structure of the 30S subunit refined to 3 Å resolution. A. The "front" or intersubunit interface side which is relatively free of proteins, with the various features of the subunit 30S labeled by their usual name. B. The "back" or solvent side, which is covered extensively by ribosomal proteins.

The structure of the 30S subunit provided a firm basis for the interpretation of decades of biochemical and genetic data (Wimberly *et al.,* 2000; Carter *et al.,* 2000; Brodersen *et al.,* 2002). The superposition of the mRNA and tRNA located in a 7.8 Å structure of the whole ribosome (Cate *et al.,* 1999), allowed us to analyze the interactions of these ligands with the 30S subunit. We were able to do this in nearly atomic detail for the P site, for a fortuitous reason: A particular feature of this crystal form was that a stem loop of 16S RNA (the "spur"; see Fig. 4) of a neighboring molecule was inserted into the P site of the 30S subunit, where it mimicked the anticodon stem loop of P-site tRNA and interacts with the 3′ end of 16S RNA which had folded back into the P site, in an analogous manner to how the tRNA anticodon interacts with the mRNA codon (Carter *et al.,* 2000).

In addition to details of the ligand binding sites, the structure revealed some very general principles. The functional sites that bound RNA ligands and the subunit interface side that formed contacts with the 50S subunit consisted almost entirely of RNA, with the exception of protein S12 near the decoding center. The active sites were highly conserved, including tertiary interactions. Many of the proteins had long extended tails at the N- or C-termini that snaked through 16S RNA and made intimate contacts with it. These features were also observed in the 50S subunit (Ban *et al.,* 2000; Nissen *et al.,* 2000). The protein-RNA interactions in the 30S subunit have been analyzed in detail (Brodersen *et al.,* 2002).

USE OF THE 30S STRUCTURE FOR THE STUDY OF ANTIBIOTIC BINDING

With a refined structure of the 30S subunit, it became straightforward directly to locate several antibiotics bound to the 30S subunit from difference Fourier maps using data collected on antibiotic complexes. Indeed, back-to-back with the 30S structure itself, we also published the structure of its complex with three different antibiotics bound simultaneously: streptomycin, spectinomycin and paromomycin (Carter *et al.*, 2000). These were followed soon afterwards by three more, tetracycline, pactamycin and hygromycin B (Brodersen *et al.*, 2000) (Fig. 5). These represented the first reports of the detailed structure of antibiotics bound to entire ribosomal subunits, although the structure of paromomycin bound to a fragment of 16S RNA containing its target had been determined previously by NMR (Fourmy *et al.*, 1996). Each of these antibiotic structures yielded insights into their respective mechanisms of action. Moreover, the detailed structure of antibiotics bound to ribosomal subunits is leading to the development of new and more effective antibiotics that may prove useful against resistant strains of pathogenic bacteria. One antibiotic, paromomycin, has also led to useful insights into decoding as discussed below.

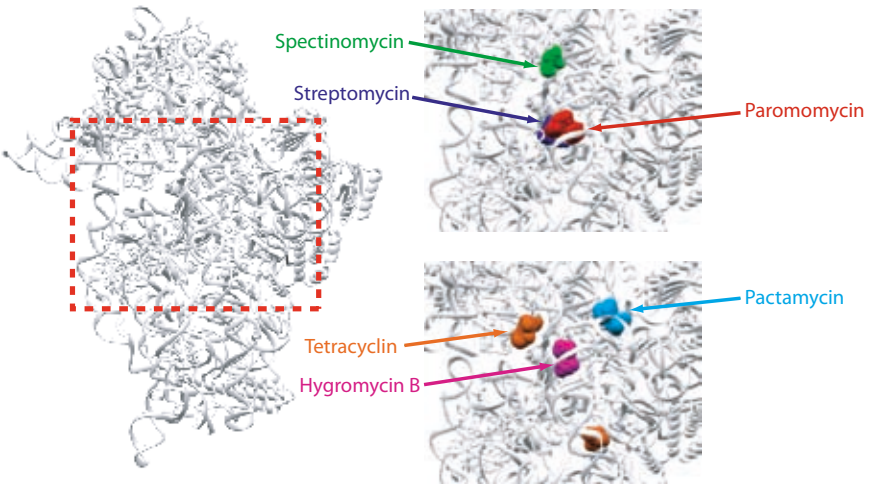

Figure 5. Antibiotics bound to the 30S subunit. The box on the left is the region of the 30S subunit where the mRNA and tRNA ligands bind, and as can be seen in the expansions of the box on the right, it is also where key antibiotics bind to key sites and cause loss of ribosome function in various ways.

THE PROBLEM OF DECODING OF THE GENETIC MESSAGE

The accuracy of translation depends on several independent processes that individually need to be at least as accurate as the overall accuracy. These processes include the recognition of the appropriate tRNA by the aminoacyl

synthetase that charges it with the correct amino acid, and maintenance of the mRNA reading frame during translation. An equally important process is decoding, which is the codon-dependent selection of the appropriate aminoacyl tRNA during protein synthesis and involves base pairing of the codon on mRNA with the anticodon on the tRNA (reviewed in Ogle and Ramakrishnan, 2005). The structure of the 30S subunit and later the entire ribosome have shed much light on decoding.

Ever since the discovery of the genetic code, it has been known that the code is highly degenerate: many codons that differ at the third position code for the same amino acid. The fact that there are fewer tRNAs than there are codons led to the wobble hypothesis in which certain kinds of mismatches are tolerated at the third or "wobble" position, whereas strict Watson-Crick pairing is required at the first two positions of the codon (Crick, 1966).

The free energy difference due to a mismatch in base pairing is not sufficient to account for the accuracy of translation. The earliest evidence that the ribosome was involved in the accuracy of tRNA selection came when the antibiotic streptomycin, which binds to the 30S subunit, was found to increase the error rate of protein synthesis (Davies *et al.,* 1964). This led to the proposal that the 30S subunit had a decoding center in which it "inspects" the pairing of a codon with an anticodon in much the same way that an enzyme senses the precise pairing of its substrate. However, this view of direct inspection ran into difficulties when a fidelity mutation, the Hirsh suppressor, was discovered at a location far from the tRNA anticodon (Hirsh, 1971), which led to the following alternative view.

Aminoacyl tRNA is initially brought into the ribosome as a complex with EF-Tu and GTP. In a view of decoding termed kinetic proofreading (Hopfield, 1974; Ninio, 1975), incorrect tRNAs can dissociate before or after GTP hydrolysis by EF-Tu. The overall selectivity can thus be as high as the product of both selection steps because they are separated by the essentially irreversible step of GTP hydrolysis. Experimental evidence for proof-reading came when it was shown that the incorporation of an amino acid by a near-cognate tRNA (which contain a single subtle mismatch between codon and anticodon) require more the hydrolysis of many more GTPs than the cognate case (Thompson and Stone, 1977; Ruusala *et al.,* 1982). In this view, both the ribosome and tRNA were passive participants in translation, with mutations altering accuracy by modulating the rate at which GTP was hydrolyzed by EF-Tu. In principle, this could explain how mutations distant from the codon-anticodon pairing could affect accuracy.

This view has required significant revision. Careful studies on the stability of RNA helices show that the free energy differences from a base-pairing mismatch can account for a factor of 5–10 in selectivity (Sugimoto *et al.,* 1986) rather than the factor of 100 assumed previously. Therefore, even with proofreading, the overall accuracy of the ribosome could not be accounted for by base-pairing alone. Pre-steady state kinetic experiments that dissected the various steps in tRNA selection showed that the *forward* rates of GTPase activation and accommodation (movement of tRNA into the peptidyl

transferase center) were dramatically higher for cognate compared to near-cognate tRNA (Pape *et al.,* 1999). This suggested that cognate tRNA more efficiently induced conformational changes in the ribosome into a productive form that accelerated GTPase activation or accommodation, consistent with earlier suggestions from NMR studies on a portion of the decoding site (Fourmy *et al.,* 1998). Several aminoglycoside antibiotics bind to the decoding center and increase the error rate of translation. Kinetic studies showed that a main effect of one such antibiotic, paromomycin, was less to increase the affinity of incorrect near-cognate tRNAs but rather to allow such tRNAs to accelerate GTPase activation (Pape *et al.,* 2000). Presumably, paromomycin induced conformational changes similar to those induced by cognate tRNAs even without the antibiotic. Subsequent equilibrium binding studies also showed that the increase in stabilization of near-cognate tRNAs due to paromomycin was minimal (Ogle *et al.,* 2002).

INSIGHTS INTO DECODING FROM STRUCTURES OF THE RIBOSOME

Possibly one of the most interesting functional insights from the structure of the 30S subunit has come from studies on codon-anticodon interactions at its decoding center. The structure has allowed a molecular explanation for the biochemical observations described above. Importantly, the structure of the 30S subunit bound to paromomycin showed that the antibiotic stabilized the conformation of two key bases, A1492 and A1493, in an orientation which suggested that they would be able to directly inspect the minor groove of the codon-anticodon helix (Carter *et al.,* 2000) (Fig. 6A and B).

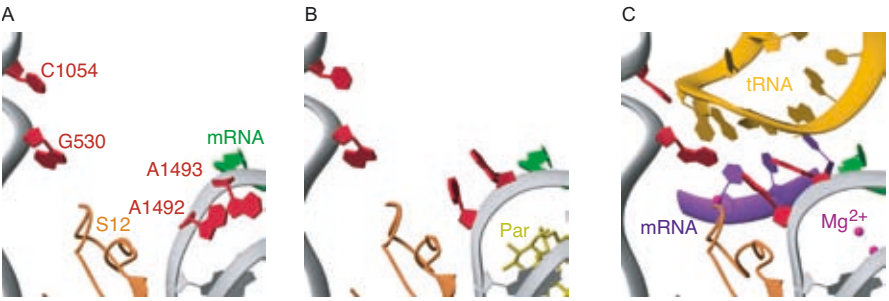

Figure 6. The decoding center of the ribosome where the mRNA codon and tRNA anticodon interact. A. The decoding center in the empty 30S subunit. B. The binding of the antibiotic paromomycin induces a conformational change in the bases A1492 and A1493, so that they are in a position to interact with the codon-anticodon base pairs. C. The base pairing between the anticodon of tRNA (whose anticodon stem-loop is shown as ASL) with the codon induces a change not only in A1492 and A1493 but also in G530 so all three bases interact with the minor groove of the codon-anticodon minihelix. Adapted from Ogle *et al.* (2001).

Testing the idea that ribosomal bases directly and specifically inspect codon-anticodon base pairing seemed difficult, because crystals would not grow

in the presence of mRNA. However we noticed that the A site of the 30S subunit where decoding occurs seemed to be exposed to large solvent channels in the crystal, suggesting that small macromolecules that bound to the A site could be soaked directly into the crystals. We tested this idea initially by soaking in the small protein initiation factor IF1, which was known to bind to the A site. We could see density for the factor in difference Fourier maps and thereby determine the structure of its complex with the 30S subunit (Carter *et al.,* 2001).

Once we knew that the A site was accessible to large ligands in the crystal, we could begin structural studies on decoding by soaking RNA oligonucleotides that mimicked the A-site mRNA codon and the tRNA anticodon stem-loop (ASL) into crystals of the 30S subunit. The data showed that the binding of cognate tRNA to the 30S subunit induced a change in the conformation not only of A1492 and A1493 but also of G530, which is part of the "530 pseudoknot" of 16S RNA (Ogle *et al.,* 2001) (Fig. 6C). These three universally conserved bases lined the minor groove of the codon-anticodon helix in such a way that the geometry of the base pair was monitored at the first two positions but not at the wobble position (Fig. 7). The structure provided a rationale for the wobble hypothesis (Crick, 1966) and the degeneracy of the code, in which strict Watson-Crick complementarity between the codon and anticodon is required at the first two positions but not the third.

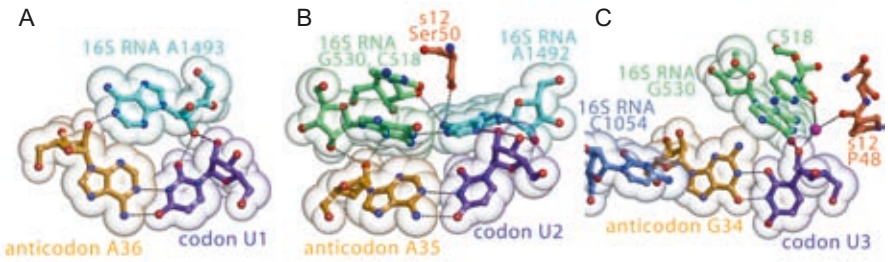

Figure 7. Interaction of conserved ribosomal bases with the three codon-anticodon base pairs showing a specific recognition of Watson-Crick geometry at the first two positions (A and B) and a tolerance of a GU wobble pair at the third position (C). Adapted from Ogle *et al.* (2001).

The binding of cognate tRNA also induced global conformational changes in the 30S subunit, in particular a movement of the shoulder of the 30S subunit relative to the rest of the body (Ogle *et al.,* 2001; Ogle *et al.,* 2002). This conformational change was not observed with near-cognate tRNA unless the antibiotic paromomycin was also present. This suggested that the conformational change induced by cognate tRNA could also be induced by near-cognate tRNA in the presence of paromomycin. Together, these structures complemented kinetic data that suggested that cognate but not near-cognate tRNA induced a conformational change that accelerated the rate of GTP hydrolysis by EF-Tu (Pape *et al.,* 1999), while paromomycin accelerated the rate of GTP hydrolysis even for near-cognate tRNA (Pape *et al.,* 2000).

A further examination of the conformational change showed that many mutations in the 30S that affected accuracy were at or near an interface between two domains of the subunit (Fig. 8). These two domains moved relative to one another upon tRNA binding in a transition from an open to a closed form of the 30S subunit. Mutations or antibiotics that made this domain closure easier lowered the accuracy of tRNA selection and those that made it more difficult to reach the closed form increased the accuracy of tRNA selection (Ogle *et al.,* 2002). The conformational changes during decoding allowed the rationalization and integration of disparate genetic and biochemical data in terms of a common mechanism (Ogle *et al.,* 2002; Ogle and Ramakrishnan, 2005).

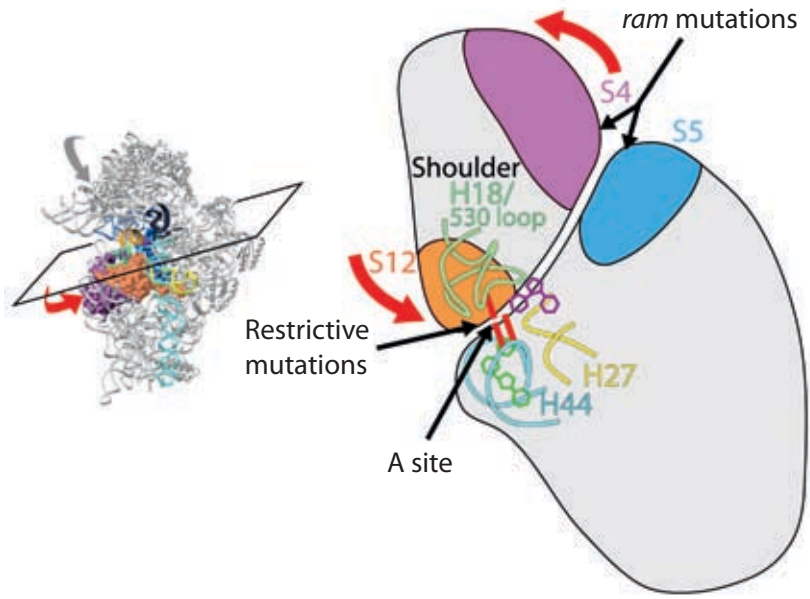

Figure 8. How conformational changes and a domain closure in the 30S ribosomal subunit can explain the effect of antibiotics or mutations on accuracy. On the right is a schematic cross-section of the 30S subunit (as shown by the plane cutting the 30S subunit on the left), in the region of the decoding center and proteins S4 (violet), S5 (blue) and S12 (orange). G530 and A1492/3 are represented by red bars; helices H44, H27 and H18 (with the G530-loop) are cyan, yellow and turquoise, respectively. The rotation of the shoulder domain (red arrows) during the transition to the closed 30S conformation disrupts an interface between S4 and S5, while the H18/530-loop/S12 region forms new contacts to H27 and H44. Mutations in these regions either increase or decrease mRNA misreading. Paromomycin (dark green rings) and streptomycin (dark pink rings) induce translational errors by facilitating domain closure. Reproduced from Ogle *et al.*(2003).

The work on the 30S subunit suggested that the domain closure from an open to a closed form was required for GTPase activation and thereby tRNA selection (Ogle *et al.,* 2002). Why should this be the case? The answer was suggested by considering domain closure in the context of cryoEM

structures of the complex of EF-Tu and tRNA bound to the ribosome (Stark *et al.,* 1997). The domain closure, in particular the movement of the shoulder of the 30S subunit, would bring the 30S closer to the EF-Tu and tRNA. We suggested that the domain closure would thereby help trigger GTP hydrolysis by EF-Tu, leading to its release and accommodation of the tRNA in the A site of the peptidyl transferase center. Subsequent cryoEM studies showed that the tRNA in complex with EF-Tu was distorted when bound to the ribosome (Valle *et al.,* 2002; Stark *et al.,* 2002). This led us to suggest a model for decoding in which the additional binding energy from the minor-groove recognition of codon-anticodon base pairing is used to induce a domain closure in the 30S subunit. This domain closure would in turn stabilize the transition state needed for GTP hydrolysis by EF-Tu, which is characterized by a distorted tRNA (Ogle *et al.,* 2002). Such a model could rationalize not only mutations in the ribosome but also those in the tRNA that affected fidelity. After GTP hydrolysis, the strong interactions at the decoding center would hold the anticodon loop in place while the release of EF-Tu would allow the highly distorted tRNA to relax into the peptidyl transferase center (Ogle *et al.,* 2002). The idea of a distorted tRNA relaxing into the peptidyl transferase center was also characterized as a "molecular spring" (Valle *et al.,* 2003), and echoes earlier ideas by Yarus and coworkers that the dynamics of tRNA were important for fidelity (Yarus and Smith, 1995).

Although the resolution of cryoEM has been steadily improving, producing structures of the 70S ribosome in complex with EF-Tu at previously unimaginable resolutions of 6–7 Å (Villa *et al.,* 2009; Schuette *et al.,* 2009), it was clear that molecular details of the interactions of EF-Tu and aminoacyl tRNA with the ribosome, and thus a further understanding of decoding, would require a higher-resolution structure. However, achieving this was slow for the reasons outlined below.

A HIGH-RESOLUTION STRUCTURE OF THE 70S RIBOSOME

The crystallization of the 70S ribosome that began in the mid-1980s in Puschino (Trakhanov *et al.,* 1987) eventually culminated in the structure of the entire 70S ribosome with mRNA and tRNA at 5.5 Å resolution (Yusupov *et al.,* 2001). This work represented a major step forward because it was the first molecular interpretation of the inter-subunit interface and the interactions of the mRNA and tRNA ligands with the ribosome. However, at that resolution, it relied on the atomic structures of the 30S and 50S subunits solved previously (Ban *et al.,* 2000; Wimberly *et al.,* 2000) to interpret the electron density in molecular terms. Indeed, those regions interpreted *ab initio* such as the L1 or L7/L12 stalks that were disordered in the 50S subunit structure proved to be incompatible with subsequent high-resolution structures of those components (Nikulin *et al.,* 2003; Diaconu *et al.,* 2005).

A second major landmark was the crystallization and structure determination of the *E. coli* ribosome at 3.5 Å resolution (Schuwirth *et al.,* 2005). This

was the first 70S ribosome structure at a resolution high enough for proper refinement of an atomic model, and among other things, resulted in a clarification of the nature of the intersubunit bridges. Moreover, because *E. coli* was the standard organism for the biochemical and genetic study of the ribosome, it was an important reference structure. Nevertheless, the crystal form was incompatible with the binding of full-length tRNAs, limiting its usefulness for functional studies. Thus it was clear that the field still needed new crystal forms of the ribosome that diffracted to high resolution in various functional states of translation.

We thus embarked on an effort to identify completely new crystal forms that would diffract well. To purify ribosomes, we again used hydrophobic chromatography as we had for the 30S subunit, but this time we used Toyopearl butyl-650S, which was suggested by Marina Garber. We found that the profile was temperature sensitive, and at 4 ˚C but not at room temperature, it was possible to separate 70S ribosomes from excess 50S subunits as well as from a fraction that contained an active ribonuclease that copurified with ribosomes. Ribosomes using our protocol also lacked any endogenously bound tRNA that might lead to heterogeneity, and were so pure that the individual charge states of whole ribosomes could be resolved by mass spectrometry (Ilag *et al.,* 2005). This led to an initial breakthrough in which we obtained a tetragonal form of the 70S ribosome, which yielded crystal structures to about 6 Å resolution of the release factors RF1 and RF2 bound to their respective stop codons on mRNA (Petry *et al.,* 2005). While these structures were a step forward, they were ultimately unsatisfying because the resolution prevented us from obtaining definitive details of the interactions of the factors with the stop codon or with the peptidyl transferase center.

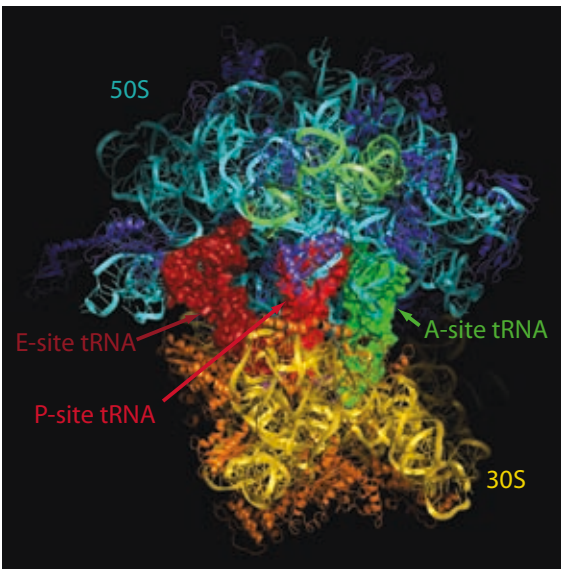

Figure 9. The entire 70S ribosome with mRNA and tRNAs, drawn from a structure at 2.8 Å (Selmer *et al.,* 2006). The short section of mRNA in this structure is barely visible in magenta because it is buried in a cleft in the 30S subunit.

In the course of trying to crystallize a complex of elongation factor G (EF-G) trapped on the ribosome by fusidic acid in the post-translocational state after GTP hydrolysis, we obtained a new orthorhombic crystal form of the ribosome that initially diffracted to about 4.5 Å resolution. However, an initial electron density map showed no evidence for EF-G in the structure, and indeed, bound EF-G would clash with a neighboring ribosome in the crystal lattice. Nevertheless, we felt this new form was sufficiently promising to continue improving, and eventually obtained a structure of the whole ribosome with mRNA and tRNA ligands at the surprisingly high resolution of 2.8 Å (Selmer *et al.,* 2006) (Figure 9). This structure provided a wealth of information about the interaction of the mRNA and tRNA ligands with the ribosome, the nature of the inter-subunit interface and the role of magnesium ions in the structure. But perhaps as important as the structure itself was the fact that this new crystal form provided a route to determine the structure of the ribosome in complex with various factors. We initially used it to solve a structure of its complex with the ribosome recycling factor RRF (Weixlbaumer *et al.,* 2007), and intermediates of the peptidyl transferase reaction (Voorhees *et al.,* 2009). Both we and the Noller laboratory used this crystal form to determine the structure of the ribosome in complex with release factors RF1 and RF2 (Laurberg *et al.,* 2008; Weixlbaumer *et al.,* 2008; Korostelev *et al.,* 2008), which shed light on translational termination. The same form has also been used in the study of elongation factor EF-P (Blaha *et al.,* 2009) and the antibiotics viomycin and capreomycin (Stanley *et al.,* 2010). Despite its general usefulness, this crystal form was not suitable for the study of GTPase factors bound to the ribosome, such as EF-G or EF-Tu because of the particular packing in the crystal lattice.

THE STRUCTURE OF THE RIBOSOME WITH GTPASE FACTORS

A characteristic of every crystal form of the ribosome previously studied was that regardless of the space group or species, protein L9 from a neighboring molecule in the lattice bound to the 30S subunit in such a way as to occlude the GTPase factor binding site. In the course of obtaining the high-resolution crystal form of the 70S ribosome described above, we learned that even with a stable complex like that of EF-G and fusidic acid with the ribosome, the L9 interaction was strong enough to displace the factor from the ribosome during crystallization. Thus over a period of many years, we were unable to obtain new crystal forms that were compatible with GTPase factor complexes of the ribosome as long as protein L9 was present. It was known that L9 was dispensable in *E. coli* (Lieberman *et al.,* 2000), so it was reasonable to assume this would also be true for *Thermus thermophilus.* Accordingly, we used genetic methods for *Thermus* (Suh *et al.,* 2005) to delete the gene for the portion of L9 that protruded out of the ribosome. Subsequently we found that not even the remaining portion of L9 was not present in ribosomes, so it was as though we had deleted the entire gene for the protein.

Our initial hope was that this mutant ribosome would still crystallize in the same form as our high-resolution crystals (Selmer *et al.,* 2006) but be able to accommodate GTPase factors. Unfortunately, the absence of L9 prevented crystallization in this form. A broad screen to search for new conditions resulted in some hits for an EF-Tu complex with the ribosome, but these were not followed up because the people involved (Frank Murphy and John Weir) both left the laboratory.

Subsequently, after new crystallization trials from scratch, we obtained a new crystal form of the EF-G fusidic acid complex with the ribosome which turned out to be in very similar conditions to the original hits for the EF-Tu complex. These crystals diffracted to about 3.5 Å resolution and resulted in a structure of the post-translational complex with EF-G (Gao *et al.,* 2009). This structure revealed many details about the interaction of EF-G with the ribosome as well as the codon and anticodon. Because fusidic acid has very low affinity for isolated EF-G, the structure also directly showed how fusidic acid binds to EF-G and locks it in a conformation that prevents its release from the ribosome.

THE STRUCTURE OF THE RIBOSOME WITH EF-TU AND AMINOACYL TRNA

The crystallization of the EF-G-fusidic acid complex with the ribosome provided the incentive to pursue the original hits with the EF-Tu-tRNA-ribosome complex. A considerable effort at optimization of these initial conditions resulted in crystals of the ternary complex bound to the ribosome stalled with kirromycin after GTP hydrolysis and the determination of its structure (Schmeing *et al.,* 2009). The overall structures of EF-G and EF-Tu bound to the ribosome are shown in Figure 10. The conformation of the factors is similar to what had been seen previously at lower resolution by cryoEM.

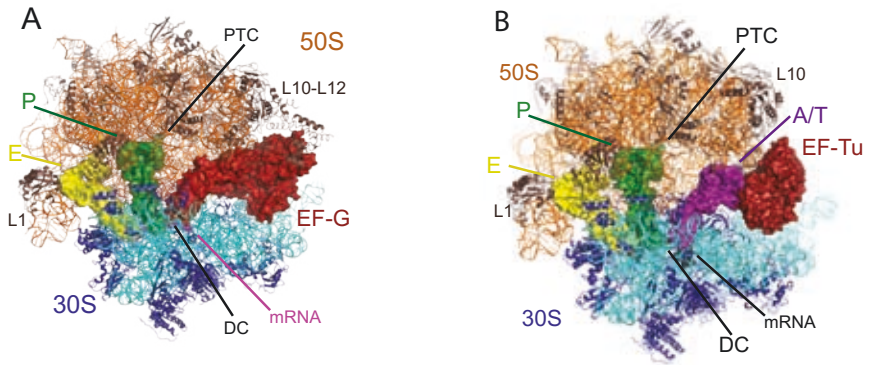

Figure 10. The structures of the GTPases EF-G (left) and EF-Tu (right) bound to the 70S ribosome (Gao *et al.,* 2009; Schmeing *et al.,* 2009). The labels refer to the peptidyl transferase center (PTC) and the decoding center (DC), E-site tRNA (E), P-site tRNA (P) and the distorted tRNA in complex with EF-Tu in the A site (A/T). The L1 and L10–L12 stalks are also indicated.

The EF-Tu-tRNA complex, in conjunction with earlier studies on the 30S subunit, provides a more complete view of the structural basis of decoding. The data suggest a sequence of events by which codon recognition eventually leads to GTP hydrolysis by EF-Tu and acceptance of the tRNA (Figure 11) (Schmeing *et al.,* 2009), that can be correlated with kinetic data (Pape *et al.,* 1998; Pape *et al.,* 1999). Recognition of the codon leads to an induced change in the three bases A1493, A1493 and G530 (Fig. 11C), which recognize the minor groove of the codon-anticodon helix as seen previously (Ogle *et al.,* 2001) This minor groove recognition stabilizes the bent form of the tRNA in the complex by helping to hold the anticodon loop tightly in the decoding center. It also induces a closing movement of the shoulder towards EF-Tu, where it interacts with a highly conserved loop of EF-Tu and thus stabilizes the factor in an altered conformation (Fig. 11D). At the same time, a base stacking interaction between the shoulder and C75 on tRNA stabilizes an altered conformation of the aminoacyl 3′ end of the tRNA. The displacement of the 3′ end of tRNA disrupts its stabilizing interactions with the crucial switch I helix of EF-Tu, which then becomes disordered, exposing the GTP to hydrolysis. Upon GTP hydrolysis, EF-Tu changes conformation to its GDP form (Jurnak, 1985; Kjeldgaard and Nyborg, 1992; Berchtold *et al.,* 1993; Kjeldgaard *et al.,* 1993). In the GDP form, it can make very few interactions with the ribosome and also has lower affinity for the tRNA, resulting in its dissociation from the ribosome and the movement of the distorted tRNA into the peptidyl transferase center (Fig. 11E).

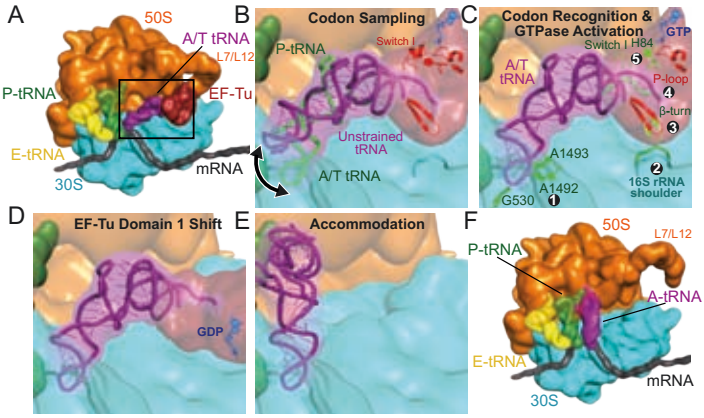

Figure 11. The decoding pathway leading to tRNA selection by the ribosome. **(A)** The L7/L12 stalk recruits the complex of EF-Tu-GTP and aminoacyltRNA to a ribosome with deacylated tRNA in the E site and peptidyl-tRNA in the P site. The black frame represents the enlarged area in panels (B)–(E). **(B)** The tRNA samples codon:anticodon pairing until a match **(C)** is sensed, by decoding center nucleotides 530 and 1492-3 ①. Codon recognition triggers domain closure of the 30S subunit ②, bringing the shoulder domain into contact with EF-Tu, and shifting the β-loop at 230–237 of domain 2 ③. This changes the conformation of the acceptor end of tRNA ④, disrupting its contacts with switch I, which becomes disordered ⑤, opening the hydrophobic gate to allow His84 to catalyze GTP hydrolysis. **(D)** GTP hydrolysis and P_i release cause domain rearrangement of EF-Tu, leading to its release from the ribosome and **(E-F)** accommodation of aminoacyl-tRNA. Reproduced from Schmeing *et al.* (2009).

FUTURE PROSPECTS

The success in the determination of the high-resolution structures of ribosomal subunits and eventually the whole ribosome was the culmination of decades of effort. It was done in the context of a large body of important work using biochemistry and genetics that provided the intellectual framework for understanding the problem. It was made possible by many technical developments, not least the development of synchrotron radiation sources, better and faster computers, better software for crystallography, and better hardware and software for visualization and interpretation of the structures. The initial structures paved the way for the structures of a number of important functional states which have shed light on the mechanisms of various aspects of translation. They have also made possible increasingly sophisticated biochemical and genetic experiments, as well as molecular dynamics studies.

Nevertheless, many important structural questions remain. In bacterial translation, a detailed visualization of the steps in initiation remains to be determined, as well as the nature of intersubunit movements that are involved in translocation (Moazed and Noller, 1989) and recycling. Understanding the interactions of the ribosome and the nascent chain with the signal recognition particle and the translocon will also be important. Beyond bacterial translation, ribosomes from eukaryotes or mitochondria remain more mysterious. In particular, understanding translational initiation in eukaryotes will benefit greatly from high-resolution structural information. In conjunction with other current work using a variety of techniques, these efforts will reveal fundamental insights into the regulation and mechanism of gene expression.

ACKNOWLEDGEMENTS

I am very grateful for the dedicated work and intellectual contributions of generations of talented postdocs, students and research assistants without whom none of the work from my laboratory would have been possible. I am also grateful for the supportive environment and great colleagues I have had at the various institutions where I have worked, including Brookhaven National Laboratory, the University of Utah and the MRC Laboratory of Molecular Biology in Cambridge. Finally, for the work described here, I am grateful for longstanding support from the U.S. National Institutes of Health and the U.K. Medical Research Council, as well as more recent support from the Wellcome Trust, the Agouron Institute and the Louis-Jeantet Foundation.

REFERENCES

1. Allen, G. S., Zavialov, A., Gursky, R., Ehrenberg, M., and Frank, J. (2005), "The cryo-EM structure of a translation initiation complex from Escherichia coli," *Cell* **121**, 703–712.
2. Ban, N., Freeborn, B., Nissen, P., Penczek, P., Grassucci, R. A., Sweet, R., Frank, J., Moore, P. B., and Steitz, T. A. (1998), "A 9 Å resolution x-ray crystallographic map of the large ribosomal subunit," *Cell* **93**, 1105–1115.
3. Ban, N., Nissen, P., Hansen, J., Moore, P. B., and Steitz, T. A. (2000), "The complete atomic structure of the large ribosomal subunit at 2.4 Å resolution," *Science* **289**, 905–920.
4. Berchtold, H., Reshetnikova, L., Reiser, C. O., Schirmer, N. K., Sprinzl, M., and Hilgenfeld, R. (1993), "Crystal structure of active elongation factor Tu reveals major domain rearrangements," *Nature* **365**, 126–132.
5. Biou, V., Shu, F., and Ramakrishnan, V. (1995), "X-ray crystallography shows that translational initiation factor IF3 consists of two compact alpha/beta domains linked by an alpha-helix," *Embo J* **14**, 4056–4064.
6. Blaha, G., Stanley, R. E., and Steitz, T. A. (2009), "Formation of the first peptide bond: the structure of EF-P bound to the 70S ribosome," *Science* **325**, 966–970.
7. Brodersen, D. E., Clemons, W. M., Jr., Carter, A. P., Morgan-Warren, R. J., Wimberly, B. T., and Ramakrishnan, V. (2000), "The structural basis for the action of the antibiotics tetracycline, pactamycin, and hygromycin B on the 30S ribosomal subunit," *Cell* **103**, 1143–1154.
8. Brodersen, D. E., Clemons, W. M., Jr., Carter, A. P., Wimberly, B. T., and Ramakrishnan, V. (2002), "Crystal structure of the 30S ribosomal subunit from *Thermus thermophilus*: Structure of the proteins and their interactions with 16S RNA," *J Mol Biol* **316**, 725–768.
9. Capel, M. S., Engelman, D. M., Freeborn, B. R., Kjeldgaard, M., Langer, J. A., Ramakrishnan, V., Schindler, D. G., Schneider, D. K., Schoenborn, B. P., Sillers, I.-Y., Yabuki, S., and Moore, P. B. (1987), "A complete mapping of the proteins in the small ribosomal subunit of *Escherichia coli," Science* **238**, 1403–1406.
10. Carter, A. P., Clemons, W. M., Jr., Brodersen, D. E., Morgan-Warren, R. J., Hartsch, T., Wimberly, B. T., and Ramakrishnan, V. (2001), "Crystal structure of an initiation factor bound to the 30S ribosomal subunit," *Science* **291**, 498–501.
11. Carter, A. P., Clemons, W. M., Jr., Brodersen, D. E., Morgan-Warren, R. J., Wimberly, B. T., and Ramakrishnan, V. (2000), "Functional insights from the structure of the 30S ribosomal subunit and its interactions with antibiotics," *Nature* **407**, 340–348.
12. Cate, J. H., Gooding, A. R., Podell, E., Zhou, K., Golden, B. L., Kundrot, C. E., Cech, T. R., and Doudna, J. A. (1996), "Crystal structure of a group I ribozyme domain: principles of RNA packing," *Science* **273**, 1678–1685.
13. Cate, J. H., Yusupov, M. M., Yusupova, G. Z., Earnest, T. N., and Noller, H. F. (1999), "X-ray crystal structures of 70S ribosome functional complexes," *Science* **285**, 2095–2104.
14. Cate, J. H., and Doudna, J. A. (1996), "Metal-binding sites in the major groove of a large ribozyme domain," *Structure* **4**, 1221–1229.
15. Chao, F. C. (1957), "Dissociation of macromolecular ribonucleoprotein of yeast," *Arch Biochem Biophys* **70**, 426–431.
16. Clemons, W. M., Jr., Brodersen, D. E., McCutcheon, J. P., May, J. L., Carter, A. P., Morgan-Warren, R. J., Wimberly, B. T., and Ramakrishnan, V. (2001), "Crystal structure of the 30S ribosomal subunit from *Thermus thermophilus*: purification, crystallization and structure determination," *J Mol Biol* **310**, 827–843.
17. Clemons, W. M., Jr., May, J. L., Wimberly, B. T., McCutcheon, J. P., Capel, M. S., and Ramakrishnan, V. (1999), "Structure of a bacterial 30S ribosomal subunit at 5.5 Å resolution," *Nature* **400**, 833–840.
18. Crick, F. H. C. (1955), "On degenerate templates and the adaptor hypothesis: a note for the RNA Tie Club" (unpublished).

19. Crick, F. H. C. (1966), "Codon-anticodon pairing: the wobble hypothesis," *J Mol Biol* **19**, 548–555.
20. Dallas, A., and Noller, H. F. (2001), "Interaction of translation initiation factor 3 with the 30S ribosomal subunit," *Molecular Cell* **8**, 855–864.
21. Davies, J., Gilbert, W., and Gorini, L. (1964), "Streptomycin, suppression, and the code," *Proc Natl Acad Sci* **51**, 883–890.
22. Diaconu, M., Kothe, U., Schlunzen, F., Fischer, N., Harms, J. M., Tonevitsky, A. G., Stark, H., Rodnina, M. V., and Wahl, M. C. (2005), "Structural basis for the function of the ribosomal L7/12 stalk in factor binding and GTPase activation," *Cell* **121**, 991–1004.
23. Dintzis, H. M. (2006), "The wandering pathway to determining the N to C synthesis of proteins," *BAMBED* **34**, 241–246.
24. Dorner, S., and Barta, A. (1999), "Probing ribosome structure by europium-induced RNA cleavage," *Biol Chem* **380**, 243–251.
25. Fourmy, D., Recht, M. I., Blanchard, S. C., and Puglisi, J. D. (1996), "Structure of the A site of *Escherichia coli* 16S ribosomal RNA complexed with an aminoglycoside antibiotic," *Science* **274**, 1367–1371.
26. Fourmy, D., Yoshizawa, S., and Puglisi, J. D. (1998), "Paromomycin binding induces a local conformational change in the A-site of 16S rRNA," *J Mol Biol* **277**, 333–345.
27. Gao, Y. G., Selmer, M., Dunham, C. M., Weixlbaumer, A., Kelley, A. C., and Ramakrishnan, V. (2009), "The structure of the ribosome with elongation factor G trapped in the posttranslocational state," *Science* **326**, 694–699.
28. Hamilton, M. G., and O'Brien, T. W. (1974), "Ultracentrifugal characterization of the mitochondrial ribosome and subribosomal particles of bovine liver: molecular size and composition," *Biochemistry* **13**, 5400–5403.
29. Hendrickson, W. A., Horton, J. R., and LeMaster, D. M. (1990), "Selenomethionyl proteins produced for analysis by multiwavelength anomalous diffraction (MAD): a vehicle for direct determination of three-dimensional structure," *Embo J* **9**, 1665–1672.
30. Hendrickson, W. A., Smith, J. L., Phizackerley, R. P., and Merritt, E. A. (1988), "Crystallographic structure analysis of lamprey hemoglobin from anomalous dispersion of synchrotron radiation," *Proteins* **4**, 77–88.
31. Hirsh, D. (1971), "Tryptophan transfer RNA as the UGA suppressor," *J Mol Biol* **58**, 439–458.
32. Hoagland, M. (2004), "Enter transfer RNA," *Nature* **431**, 249.
33. Hoagland, M. B., Stephenson, M. L., Scott, H. F., Hecht, L. I., and Zamecnik, P. C. (1958), "A soluble ribonucleic acid intermediate in protein synthesis," *J Biol Chem* **231**, 241–257.
34. Holley, R. W., Apgar, J., Everett, G. A., Madison, J. T., Marquisee, M., Merrill, S. H., Penswick, J. R., and Zamir, A. (1965), "Structure of a Ribonucleic Acid," *Science* **147**, 1462–1465.
35. Hope, H. (1988), "Cryocrystallography of biological macromolecules: A generally applicable method," *Acta Crystallogr* **B 44**, 22–26.
36. Hope, H., Frolow, F., von Böhlen, K., Makowski, I., Kratky, C., Halfon, Y., Danz, H., Webster, P., Bartels, K. S., Wittmann, H. G., and Yonath, A. (1989), "Cryocrystallography of ribosomal particles," *Acta Crystallogr* **B 45**, 190–199.
37. Hopfield, J. J. (1974), "Kinetic proofreading: a new mechanism for reducing errors in biosynthetic processes requiring high specificity," *Proc Natl Acad Sci* **71**, 4135–4139.
38. Ilag, L. L., Videler, H., McKay, A. R., Sobott, F., Fucini, P., Nierhaus, K. H., and Robinson, C. V. (2005), "Heptameric (L12)6/L10 rather than canonical pentameric complexes are found by tandem MS of intact ribosomes from thermophilic bacteria," *Proc Natl Acad Sci U S A* **102**, 8192–8197.
39. Jurnak, F. (1985), "Structure of the GDP domain of EF-Tu and location of the amino acids homologous to ras oncogene proteins," *Science* **230**, 32–36.
40. Kim, S. H., Suddath, F. L., Quigley, G. J., McPherson, A., Sussman, J. L., Wang, A. H.,

Seeman, N. C., and Rich, A. (1974), "Three-dimensional tertiary structure of yeast phenylalanine transfer RNA," *Science* **185**, 435–440.
41. Kjeldgaard, M., Nissen, P., Thirup, S., and Nyborg, J. (1993), "The crystal structure of elongation factor EF-Tu from *Thermus aquaticus* in the GTP conformation," *Structure* **1**, 35–50.
42. Kjeldgaard, M., and Nyborg, J. (1992), "Refined structure of elongation factor EF-Tu from *Escherichia coli*," *J Mol Biol* **223**, 721–742.
43. Korostelev, A., Asahara, H., Lancaster, L., Laurberg, M., Hirschi, A., Zhu, J., Trakhanov, S., Scott, W. G., and Noller, H. F. (2008), "Crystal structure of a translation termination complex formed with release factor RF2," *Proc Natl Acad Sci U S A* **105**, 19684–19689.
44. Lata, K. R., Agrawal, R. K., Penczek, P., Grassucci, R., Zhu, J., and Frank, J. (1996), "Three-dimensional reconstruction of the *Escherichia coli* 30S ribosomal subunit in ice," *J Mol Biol* **262**, 43–52.
45. Laurberg, M., Asahara, H., Korostelev, A., Zhu, J., Trakhanov, S., and Noller, H. F. (2008), "Structural basis for translation termination on the 70S ribosome," *Nature* **454**, 852–857.
46. Lieberman, K. R., Firpo, M. A., Herr, A. J., Nguyenle, T., Atkins, J. F., Gesteland, R. F., and Noller, H. F. (2000), "The 23 S rRNA environment of ribosomal protein L9 in the 50 S ribosomal subunit," *J Mol Biol* **297**, 1129–1143.
47. Lindahl, M., Svensson, L. A., Liljas, A., Sedelnikova, S. E., Eliseikina, I. A., Fomenkova, N. P., Nevskaya, N., Nikonov, S. V., Garber, M. B., Muranova, T. A., Rykonova, A. I., and Amons, R. (1994), "Crystal structure of the ribosomal protein S6 from *Thermus thermophilus*," *Embo J* **13**, 1249–1254.
48. Liu, Y., Ogata, C. M., and Hendrickson, W. A. (2001), "Multiwavelength anomalous diffraction analysis at the M absorption edges of uranium," *Proc Natl Acad Sci U S A* **98**, 10648–10653.
49. McCutcheon, J. P., Agrawal, R. K., Philips, S. M., Grassucci, R. A., Gerchman, S. E., Clemons, W. M., Jr., Ramakrishnan, V., and Frank, J. (1999), "Location of translation al initiation factor IF3 on the small ribosomal subunit," *Proc Natl Acad Sci* **96**, 4301–4306.
50. Moazed, D., and Noller, H. F. (1989), "Intermediate states in the movement of transfer RNA in the ribosome," *Nature* **342**, 142–148.
51. Nikulin, A., Eliseikina, I., Tishchenko, S., Nevskaya, N., Davydova, N., Platonova, O., Piendl, W., Selmer, M., Liljas, A., Drygin, D., Zimmermann, R., Garber, M., and Nikonov, S. (2003), "Structure of the L1 protuberance in the ribosome," *Nat Struct Biol.* **10**, 104–108.
52. Ninio, J. (1975), "Kinetic amplification of enzyme discrimination," *Biochimie* **57**, 587–595.
53. Nissen, P., Hansen, J., Ban, N., Moore, P. B., and Steitz, T. A. (2000), "The structural basis of ribosome activity in peptide bond synthesis," *Science* **289**, 920–930.
54. Nomura, M., Tissières, A., and Lengyel, P. (1974), *Ribosomes* (New York: Cold Spring Harbor Monograph Series).
55. Ogle, J. M., Brodersen, D. E., Clemons, W. M., Jr., Tarry, M. J., Carter, A. P., and Ramakrishnan, V. (2001), "Recognition of cognate transfer RNA by the 30S ribosomal subunit," *Science* **292**, 897–902.
56. Ogle, J. M., Carter, A. P., and Ramakrishnan, V. (2003), "Insights into the decoding mechanism from recent ribosome structures," *Trends Biochem Sci* **28**, 259–266.
57. Ogle, J. M., Murphy, F. V., Tarry, M. J., and Ramakrishnan, V. (2002), "Selection of tRNA by the ribosome requires a transition from an open to a closed form," *Cell* **111**, 721–732.
58. Ogle, J. M., and Ramakrishnan, V. (2005), "Structural Insights into Translational Fidelity," *Ann Rev Biochem* **74**, 129–177.
59. Palade, G. E., and Siekevitz, P. (1956), "Pancreatic microsomes; an integrated morphological and biochemical study," *J Biophys Biochem Cytol* **2**, 671–690.

60. Pape, T., Wintermeyer, W., and Rodnina, M. (1999), "Induced fit in initial selection and proofreading of aminoacyl-tRNA on the ribosome," *Embo J* **18**, 3800–3807.
61. Pape, T., Wintermeyer, W., and Rodnina, M. V. (1998), "Complete kinetic mechanism of elongation factor Tu-dependent binding of aminoacyl-tRNA to the A site of the *E. coli* ribosome," *Embo J* **17**, 7490–7497.
62. Pape, T., Wintermeyer, W., and Rodnina, M. V. (2000), "Conformational switch in the decoding region of 16S rRNA during aminoacyl-tRNA selection on the ribosome," *Nat Struct Biol* **7**, 104–107.
63. Petry, S., Brodersen, D. E., Murphy, F. V. t., Dunham, C. M., Selmer, M., Tarry, M. J., Kelley, A. C., and Ramakrishnan, V. (2005), "Crystal structures of the ribosome in complex with release factors RF1 and RF2 bound to a cognate stop codon," *Cell* **123**, 1255–1266.
64. Phillips, J. C., and Hodgson, K. O. (1980), "The use of anomalous scattering effects to phase diffraction patterns from macromolecules," *Acta Cryst* **A36**, 856–864.
65. Pioletti, M., Schlunzen, F., Harms, J., Zarivach, R., Gluhmann, M., Avila, H., Bashan, A., Bartels, H., Auerbach, T., Jacobi, C., Hartsch, T., Yonath, A., and Franceschi, F. (2001), "Crystal structures of complexes of the small ribosomal subunit with tetracycline, edeine and IF3," *Embo J* **20**, 1829–1839.
66. Powers, T., and Noller, H. F. (1995), "Hydroxyl radical footprinting of ribosomal proteins on 16S rRNA," *RNA* **1**, 194–209.
67. Ramakrishnan, V., and Biou, V. (1997), "Treatment of multiwavelength anomalous diffraction data as a special case of multiple isomorphous replacement," In *Meth Enzymol*, Carter, C. W., Jr., and R. M. Sweet, eds. (New York: Academic Press), pp. 538–557.
68. Ramakrishnan, V., Finch, J. T., Graziano, V., Lee, P. L., and Sweet, R. M. (1993), "Crystal structure of globular domain of histone H5 and its implications for nucleosome binding," *Nature* **362**, 219–223.
69. Ramakrishnan, V., and Gerchman, S. E. (1991), "Cloning, sequencing and overexpression of genes for ribosomal proteins from *Bacillus stearothermophilus*," *J Biol Chem* **266**, 880–885.
70. Ramakrishnan, V., Graziano, V., and Capel, M. S. (1986), "A role for proteins S3 and S14 in the 30S ribosomal subunit," *J Biol Chem* **261**, 15049–15052.
71. Ramakrishnan, V., and White, S. W. (1998), "Ribosomal protein structures: insights into the architecture, machinery and evolution of the ribosome," *Trends Biochem Sci* **23**, 208–212.
72. Robertus, J. D., Ladner, J. E., Finch, J. T., Rhodes, D., Brown, R. S., Clark, B. F., and Klug, A. (1974), "Structure of yeast phenylalanine tRNA at 3 Å resolution," *Nature* **250**, 546–551.
73. Ruusala, T., Ehrenberg, M., and Kurland, C. G. (1982), "Is there proofreading during polypeptide synthesis?" *Embo J* **1**, 741–745.
74. Schluenzen, F., Tocilj, A., Zarivach, R., Harms, J., Gluehmann, M., Janell, D., Bashan, A., Bartels, H., Agmon, I., Franceschi, F., and Yonath, A. (2000), "Structure of functionally activated small ribosomal subunit at 3.3 angstroms resolution," *Cell* **102**, 615–623.
75. Schmeing, T. M., Voorhees, R. M., Kelley, A. C., Gao, Y. G., Murphy, F. V. t., Weir, J. R., and Ramakrishnan, V. (2009), "The crystal structure of the ribosome bound to EF-Tu and aminoacyl-tRNA," *Science* **326**, 688–694.
76. Schuette, J. C., Murphy, F. V. t., Kelley, A. C., Weir, J. R., Giesebrecht, J., Connell, S. R., Loerke, J., Mielke, T., Zhang, W., Penczek, P. A., Ramakrishnan, V., and Spahn, C. M. (2009), "GTPase activation of elongation factor EF-Tu by the ribosome during decoding," *Embo J* **28**, 755–765.
77. Schuwirth, B. S., Borovinskaya, M. A., Hau, C. W., Zhang, W., Vila-Sanjurjo, A., Holton, J. M., and Cate, J. H. (2005), "Structures of the bacterial ribosome at 3.5 A resolution," *Science* **310**, 827–834.
78. Selmer, M., Dunham, C. M., Murphy, F. V. t., Weixlbaumer, A., Petry, S., Kelley, A. C.,

Weir, J. R., and Ramakrishnan, V. (2006), "Structure of the 70S ribosome complexed with mRNA and tRNA," *Science* **313**, 1935–1942.
79. Stanley, R. E., Blaha, G., Grodzicki, R. L., Strickler, M. D., and Steitz, T. A. (2010), "The structures of the anti-tuberculosis antibiotics viomycin and capreomycin bound to the 70S ribosome," *Nat Struct Mol Biol*
80. Stark, H., Rodnina, M. V., Rinke-Appel, J., Brimacombe, R., Wintermeyer, W., and van Heel, M. (1997), "Visualization of elongation factor Tu on the *Escherichia coli* ribosome," *Nature* **389**, 403–406.
81. Stark, H., Rodnina, M. V., Wieden, H. J., Zemlin, F., Wintermeyer, W., and Van Heel, M. (2002), "Ribosome interactions of aminoacyl-tRNA and elongation factor Tu in the codon-recognition complex," *Nat Struct Biol* **9**, 849–854.
82. Stern, S., Powers, T., Changchien, L. M., and Noller, H. F. (1989), "RNA-protein interactions in 30S ribosomal subunits: folding and function of 16S rRNA," *Science* **244**, 783–790.
83. Studier, F. W., Rosenberg, A. H., Dunn, J. J., and Dubendorff, J. W. (1990), "Use of T7 RNA polymerase to direct expression of cloned genes," *Meth Enzymol* **185**, 61–89.
84. Sugimoto, N., Kierzek, R., Freier, S. M., and Turner, D. H. (1986), "Energetics of internal GU mismatches in ribooligonucleotide helixes," *Biochemistry* **25**, 5755–5759.
85. Suh, M. J., Hamburg, D. M., Gregory, S. T., Dahlberg, A. E., and Limbach, P. A. (2005), "Extending ribosomal protein identifications to unsequenced bacterial strains using matrix-assisted laser desorption/ionization mass spectrometry," *Proteomics* **5**, 4818–4831.
86. Thompson, R. C., and Stone, P. J. (1977)," Proofreading of the codon-anticodon interaction on ribosomes," *Proc Natl Acad Sci* **74**, 198–202.
87. Thygesen, J., Weinstein, S., Franceschi, F., and Yonath, A. (1996), "The suitability of multi-metal clusters for phasing in crystallography of large macromolecular assemblies," *Structure* **4**, 513–518.
88. Tissières, A., and Watson, J. D. (1958), "Ribonucleoprotein particles from *Escherichia coli*," *Nature* **182**, 778–780.
89. Trakhanov, S. D., Yusupov, M. M., Agalarov, S. C., Garber, M. B., Ryazantsev, S. N., Tischenko, S. V., and Shirokov, V. A. (1987), "Crystallization of 70 S ribosomes and 30S ribosomal subunits from *Thermus thermophilus*," *FEBS Lett* **220**, 319–322.
90. Unwin, P. N., and Taddei, C. (1977), "Packing of ribosomes in crystals from the lizard Lacerta sicula," *J Mol Biol* **114**, 491–506.
91. Valle, M., Sengupta, J., Swami, N. K., Grassucci, R. A., Burkhardt, N., Nierhaus, K. H., Agrawal, R. K., and Frank, J. (2002), "Cryo-EM reveals an active role for aminoacyl-tRNA in the accommodation process," *Embo J* **21**, 3557–3567.
92. Valle, M., Zavialov, A., Li, W., Stagg, S. M., Sengupta, J., Nielsen, R. C., Nissen, P., Harvey, S. C., Ehrenberg, M., and Frank, J. (2003), "Incorporation of aminoacyltRNA into the ribosome as seen by cryo-electron microscopy," *Nat Struct Biol* **10**, 899–906.
93. Villa, E., Sengupta, J., Trabuco, L. G., LeBarron, J., Baxter, W. T., Shaikh, T. R., Grassucci, R. A., Nissen, P., Ehrenberg, M., Schulten, K., and Frank, J. (2009), "Ribosome-induced changes in elongation factor Tu conformation control GTP hydrolysis," *Proc Natl Acad Sci U S A* **106**, 1063–1068.
94. von Böhlen, K., Makowski, I., Hansen, H. A. S., Bartels, H., Berkovitch-Yellin, Z., Zaytzev-Bashan, A., Meyer, S., Paulke, C., Franceschi, F., and Yonath, A. (1991), "Characterization and preliminary attempts for derivatization of crystals of large ribosomal subunits from *Haloarcula marismortui* diffracting to 3 Å resolution," *J Mol Biol* **222**, 11–15.
95. Voorhees, R. M., Weixlbaumer, A., Loakes, D., Kelley, A. C., and Ramakrishnan, V. (2009), "Insights into substrate stabilization from snapshots of the peptidyl transferase center of the intact 70S ribosome," *Nat Struct Mol Biol* **16**, 528–533.
96. Weis, W. I., Kahn, R., Fourme, R., Drickamer, K., and Hendrickson, W. A. (1991),

"Structure of the calcium-dependent lectin domain from a rat mannose-binding protein determined by MAD phasing," *Science* **254**, 1608–1615.
97. Weixlbaumer, A., Jin, H., Neubauer, C., Voorhees, R. M., Petry, S., Kelley, A. C., and Ramakrishnan, V. (2008), "Insights into translational termination from the structure of RF2 bound to the ribosome," *Science* **322**, 953–956.
98. Weixlbaumer, A., Petry, S., Dunham, C. M., Selmer, M., Kelley, A. C., and Ramakrishnan, V. (2007), "Crystal structure of the ribosome recycling factor bound to the ribosome," *Nat Struct Mol Biol* **14**, 733–737.
99. Wimberly, B. T., Brodersen, D. E., Clemons, W. M., Jr., Morgan-Warren, R. J., Carter, A. P., Vonrhein, C., Hartsch, T., and Ramakrishnan, V. (2000), "Structure of the 30S ribosomal subunit," *Nature* **407**, 327–339.
100. Yarus, M., and Smith, D. (1995), "tRNA on the ribosome: a waggle theory," in *tRNA: Structure, biosynthesis and function*, Söll, D., and U. RajBhandary, eds. (Washington: American Society for Microbiology Press), pp. 443–468.
101. Yonath, A., Glotz, C., Gewitz, H. S., Bartels, K. S., von Böhlen, K., Makowski, L., and Wittmann, H. G. (1988), "Characterization of crystals of small ribosomal subunits," *J Mol Biol* **203**, 831–834.
102. Yonath, A., Mussig, J., Tesche, B., Lorenz, S., Erdmann, V. A., and Wittmann, H. G. (1980), "Crystallization of the large ribosomal subunits from *Bacillus stearothermophilus*," *Biochem Int* **1**, 428–435.
103. Yusupov, M. M., Trakhanov, S. D., Barynin, V. V., Borovyagin, V. L., Garber, M. B., Sedelnikova, O. M., Tishchenko, S. V., and Shirokov, V. A. (1987), "Crystallization of 30S ribosomal subunits from *T. thermophilus*," *Dokl Akad Nauk USSR* **292**, 1271–1274.
104. Yusupov, M. M., Yusupova, G. Z., Baucom, A., Lieberman, K., Earnest, T. N., Cate, J. H., and Noller, H. F. (2001), "Crystal structure of the ribosome at 5.5 A resolution," *Science* **292**, 883–896.

Portrait photo of Dr. Ramakrishnan by photographer Ulla Montan.